

Fracture properties of steel fibre reinforced high-performance concrete containing nano-SiO₂ and fly ash

Peng Zhang*, Chen-Hui Liu, Qing-Fu Li, Tian-Hang Zhang and Peng Wang

School of Water Conservancy and Environment Engineering, Zhengzhou University, Zhengzhou 450001, China

In this article, we study the effect of steel fibre on the fracture properties of high performance concrete (HPC) containing fly ash and nano-SiO₂. The results reveal that the addition of appropriate content of steel fibre helps improve the fracture properties of HPC. Steel fibre improves the fracture parameters of initial fracture toughness, unstable fracture toughness, fracture energy and critical crack opening displacement of the beam specimen of HPC. The results also show that steel fibre has major effect on the fracture curves of the three-point bending beam specimen. The fracture toughness and fracture energy increase gradually, and the area under the fracture relational curve becomes larger when the steel fibre content increases from 0.5% to 2%. However, these fracture parameters begin to decrease and the area under the fracture relational curve becomes smaller when the steel fibre content exceeds 2%. This indicates that steel fibre helps improve the fracture properties of HPC containing nano-SiO₂ and fly ash only when its fibre content does not exceed 2%.

Keywords: Fly ash, fracture properties, high performance concrete, nano-SiO₂, steel fibre.

HIGH performance concrete (HPC) is widely used in civil engineering with the development of concrete technology. In addition to the three basic ingredients in conventional concrete, i.e. Portland cement, fine and coarse aggregates and water, HPC incorporates supplementary cementitious materials such as fly ash and blast furnace slag, and chemical admixture such as superplasticizer¹. HPC is concrete which meets the special performance and uniformity requirements that cannot always be achieved by conventional materials, normal mixing, placing and curing practices². According to Swamy³, HPC is designed to give optimized performance characteristics for a given set of materials, usage and exposure conditions, consistent with requirements of cost, service life and durability. A large number of researchers have studied the mechanical properties, fracture properties and durability of HPC, and their study results indicate that it shows better

mechanical properties, fracture properties and durability compared to conventional concrete⁴⁻⁹.

In addition to the three basic ingredients, i.e. cement, aggregates and water used in conventional concrete, active mineral additives like fly ash¹⁰, blast furnace slag¹¹, rice husk ash¹² and silica fume¹³ have been incorporated to make HPC. Today, nanotechnology has attracted considerable interest due to the new potential uses of particles in nanometre scale. Nanotechnology encompasses the techniques of manipulation of the structure at the nanometre scale to develop a new generation of tailored, multifunctional, cementitious composites with superior mechanical performance and durability potentially having a range of novel properties such as low electrical resistivity, self-sensing capabilities, self-cleaning, self-healing, high ductility and self-control of cracks¹⁴. As a result, nanoparticles have been used in concrete engineering with the rapid development of nanotechnology. There are several kinds of nanoparticles often used in concrete: nano-SiO₂, nano-CaCO₃, nano-Al₂O₃, nano-TiO₂, nano-ZnO₂ and nano-ZrO₂; nano-SiO₂ seems to be the most popular among the researchers¹⁵⁻²⁰. In the last few years, several researchers have studied the effect of nano-SiO₂ on the performance of concrete²¹⁻²⁴ and their results indicate that the mechanical properties and durability of concrete are greatly improved with the addition of nano-SiO₂.

Although there is great improvement in many aspects of material properties for concrete with the addition of nanoparticles, the toughness of concrete reinforced with nanoparticles, which is beneficial for the safety of concrete structures, still needs to be improved. In the last few decades, various kinds of fibres have been applied to improve the toughness and crack resistance of concrete. Numerous types of fibre are available for commercial use in concrete, the basic types being steel, glass, synthetic materials and some natural fibres²⁵. Among these fibres, steel fibre is the most popular and widely used in both research and practice. Nowadays, steel fibre reinforced concrete has been successfully used in several types of construction due to the fact that steel fibres improve the durability and mechanical properties of hardened concrete, namely flexural strength, toughness, impact strength, resistance to fatigue, vulnerability to cracking and spalling.

*For correspondence. (e-mail: zhangpeng8008@gmail.com)

Fracture properties are extremely important for the safety and durability of concrete. However, little information is presently available regarding the influence of steel fibre on the fracture properties of SiO₂ nanoparticles reinforced HPC. Therefore, we conducted the present experimental study and measured the fracture toughness, fracture energy, mid-span deflection (δ), crack mouth opening displacement (CMOD) and crack tip opening displacement (CTOD) of the notched beam specimens of steel fibre reinforced HPC containing nano-SiO₂ to observe the effect of steel fibre on fracture properties of concrete containing nano-SiO₂.

Experimental procedure

Raw materials

The cement used was Ordinary Portland cement (Class 42.5R) whose chemical and physical properties are presented in Table 1. Grade I fly ash was used to make HPC whose chemical properties are also presented in Table 1. In this study, amorphous nano-SiO₂ with a solid content of more than 99% was used. Physical properties of the nanoparticles are presented in Table 2. Physical properties of mill-cut steel fibres are presented in Table 3. Coarse aggregate with a maximum size of 20 mm and fine aggregate with a 2.76 fineness modulus were used. A high-range water-reducing agent with commercial name 'polycarboxylate HJSX-A' was used to adjust the workability of the concrete mixture. The performance indices of the high-range water-reducing agent are presented in Table 4. Mix proportions of the concrete composites are given in Table 5.

Table 1. Properties of cement and fly ash

Composition (%)	Cement	Fly ash
Chemical composition		
SiO ₂	20.85	51.50
Al ₂ O ₃	5.32	18.46
Fe ₂ O ₃	2.69	6.71
CaO	62.97	8.58
MgO	3.66	3.93
Na ₂ O	0.15	2.52
K ₂ O	0.62	1.85
SO ₃	2.48	0.21
Physical properties		
Specific gravity	3.11	2.16
Specific surface (cm ² /g)	3287	2470

Table 2. Physical properties of nano-SiO₂

Average particle size (nm)	SiO ₂ content (%)	Specific surface area (m ² /g)	Apparent density (g/cm ³)	pH value
30	99.5	200 ± 10	0.055	5–7

Preparation of specimens

A series of notched beam specimens with the size of 100 × 100 × 515 mm were prepared to determine the fracture properties. The beam specimen was sawed from the span centre of the lower surface to produce a pre-cutting crack, the depth of which is 40 mm. The shape and size of the beam specimen are shown in Figure 1. In order to distribute nano-SiO₂ uniformly, a forced mixing machine was used. The mixing procedure, which was designed by trial and error, was chosen as follows: the coarse aggregate and fine aggregate were mixed initially for 1 min, and then steel fibres were mixed for another 1 min, and the cement, fly ash and nano-SiO₂ were mixed for another 2 min. Finally, the high-range water-reducing agent and water were added and mixed for 3 min. After casting, all the specimens were finished with a steel towel. Immediately after finishing, the specimens were covered with plastic sheets to minimize moisture loss from them. They were stored at a temperature of about 23°C in casting room. The specimens were demoulded after 24 h and then cured at 100% relative humidity and controlled temperature (21 ± 2°C) for 28 days before testing.

Fracture test method

Three-point bending beam method was employed to measure the fracture parameters in the present study, which is an appropriate fracture testing method recommended by the Committee on Fracture Mechanics of Concrete of the International Union of Laboratories and Experts in Construction Materials, Systems and Structures²⁶. The experiment was carried out on a hydraulic pressure testing machine, whose measure range of the load transducer is 0–30 kN. CMOD and CTOD were measured by clamp-type extended instruments. δ of the beam specimen was measured using a displacement meter fixed on one side face of the specimen using an angle bracket. During the course of testing, the loading was kept continual and consistent, and the loading rate was reduced properly when the specimen was approaching

Table 3. Properties of steel fibres

Length (mm)	Equivalent diameter (mm)	Length : diameter ratio	Tensile strength (MPa)
32	0.56	52.0	800

Table 4. Properties of high-range water-reducing agent

Solid content (%)	Total alkali content (%)	Fluidity of cement paste (mm)	Density (g/cm ³)	Content of CF (%)	pH value
30	1.2	260	1.052	0.078	4.32

Table 5. Mix proportions of high performance concrete

Mix no.	Cement (kg/m ³)	Fly ash (%)	Nano-SiO ₂ (%)	Steel fibre (%)	Fine aggregate (kg/m ³)	Coarse aggregate (kg/m ³)	Water (kg/m ³)	Water-reducing agent (kg/m ³)
1	395.2	15	5	0.5	647	1151	158	4.94
2	395.2	15	5	1	647	1151	158	4.94
3	395.2	15	5	1.5	647	1151	158	4.94
4	395.2	15	5	2	647	1151	158	4.94
5	395.2	15	5	2.5	647	1151	158	4.94

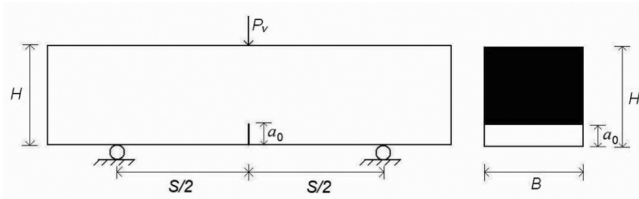


Figure 1. Sketch of three-point bending beam specimen.



Figure 2. Loading device of three-point bending test.

failure. The relational curves between the vertical load and the mid-span deflection ($P_v-\delta$), crack mouth opening displacement (P_v -CMOD), and crack tip opening displacement (P_v -CTOD) were obtained respectively from the X-Y dynamic function recorder. The testing apparatus of the fracture test is shown in Figure 2.

Determination of fracture parameters

In this study, the fracture properties of HPC were evaluated by the double-K fracture parameters (initial fracture toughness K_{IC}^{ini} and unstable fracture toughness K_{IC}^{un})²⁷, and fracture energy G_F . Here the propagation length of the crack is needed for the calculation of K_{IC}^{ini} and K_{IC}^{un} . The higher K_{IC}^{ini} and K_{IC}^{un} indicate that concrete is more resistant to crack expansion and it has better fracture properties. The effective crack length of the

three-point bending beam specimen is generally used to calculate K_{IC}^{ini} and K_{IC}^{un} , and the effective crack length can be calculated as follows²⁸

$$a_c = \frac{2}{\pi} H \times \arctan \sqrt{\frac{EB}{32.6 P_{Vmax}} CMOD_c - 0.1135}, \tag{1}$$

where a_c is the effective crack length of the three-point bending beam specimen (m); P_{Vmax} the peak vertical load (kN); $CMOD_c$ the critical crack mouth opening displacement (m); E the elastic modulus of the concrete composite (MPa); H the height of the beam specimen (m); and B the width of the beam specimen (m).

With the measured initial cracking load and depth of the pre-cutting crack of the three-point bending beam specimen, the initial fracture toughness of concrete composite containing nano-SiO₂ can be calculated as follows²⁹

$$K_{IC}^{ini} = \frac{3 P_{ini} S \sqrt{a_0}}{2 B H^2} f\left(\frac{a_0}{H}\right), \tag{2}$$

where K_{IC}^{ini} is the initial fracture toughness (kN/m^{3/2}); P_{ini} the initial cracking load (kN); S the span length of the beam specimen (m); H the height of the beam specimen (m); B the width of the beam specimen (m); and a_0 the depth of the pre-cutting crack of the three-point bending beam specimen (m).

$$f\left(\frac{a_0}{H}\right) = \frac{1.99 - \frac{a_0}{H} \left(1 - \frac{a_0}{H}\right) \left[2.15 - 3.93 \frac{a_0}{H} + 2.7 \left(\frac{a_0}{H}\right)^2\right]}{\left(1 + 2 \frac{a_0}{H}\right) \left(1 - \frac{a_0}{H}\right)^{1.5}}. \tag{3}$$

With the measured peak vertical load and the effective crack length of the three-point bending beam specimen, the unstable fracture toughness of concrete composite containing nano-SiO₂ can be calculated as follows²⁹

$$K_{IC}^{un} = \frac{3 P_{Vmax} S \sqrt{a_c}}{2 B H^2} f\left(\frac{a_c}{H}\right), \tag{4}$$

where K_{IC}^{un} is the unstable fracture toughness ($\text{kN/m}^{3/2}$); P_{Vmax} the peak vertical load (kN); S the span length of the beam specimen (m); H the height of the beam specimen (m); B the width of the beam specimen (m); and a_c the effective crack length of the three-point bending beam specimen (m).

$$f\left(\frac{a_c}{H}\right) = \frac{1.99 - \frac{a_c}{H} \left(1 - \frac{a_c}{H}\right) \left[2.15 - 3.93 \frac{a_c}{H} + 2.7 \left(\frac{a_c}{H}\right)^2\right]}{\left(1 + 2 \frac{a_c}{H}\right) \left(1 - \frac{a_c}{H}\right)^{1.5}} \quad (5)$$

The fracture energy results from integration of the load–displacement curve per unit of the fractured surface of the specimen³⁰. With the measured ultimate mid-span deflection and the relational curve of $P_V-\delta$ of the three-point bending beam specimen, the fracture energy of steel fibre reinforced HPC containing nano-SiO₂ can be calculated as follows³¹

$$G_F = \frac{1}{A_{lig}} [W_0 + (m_1 + 2m_2)g\delta_{max}] \quad (6)$$

$$A_{lig} = B(H - a_0) \quad (7)$$

where G_F is the fracture energy (N/m); A_{lig} the area of the fracture ligament of the specimen (m^2); H the height of the beam specimen (m); B the width of the beam specimen (m); a_0 the depth of the notched crack (m); g the gravitational acceleration ($= 9.8 \text{ m/s}^2$); m_1 the weight of the specimen between the two supports (kg); m_2 the additive weight of the loading facilities (kg); δ_{max} the maximum mid-span deflection of the beam specimen (m); W_0 the area above the axis of δ and under the relational curve of $P_V-\delta$ shown in Figure 3 (N·m). There are six specimens for each proportion, and the average of the six values is taken as the final result.

Results and discussion

Effect of steel fibre on compressive and flexural strength

Figure 4 *a* and *b* illustrates the variation of compressive strength and flexural strength respectively of steel fibre reinforced HPC containing 5% nano-SiO₂ and 15% fly ash with the steel fibre content increasing from 0.5% to 2.5% at 28 days curing period. From the figure, it can be seen that steel fibre content has a major effect on the strength of concrete containing nanoparticles and fly ash. Both the compressive strength and flexural strength increase gradually with increase in steel fibre content from

0.5% to 2%, whereas they begin to decrease when the steel fibre content exceeds 2%. The interface adhesive property between the concrete matrix and steel fibre was strengthened with the addition of nanoparticles. The load can be transmitted to the steel fibres through the concrete matrix and the matrix can bear the load together with the steel fibres. As a result, both the compressive and flexural strength improved with the appropriate steel fibre content.

Effect of steel fibre on fracture toughness

Figure 5 *a* and *b* shows the variation of initial fracture toughness (K_{IC}^{ini}) and unstable fracture toughness (K_{IC}^{un}) respectively, of HPC containing 5% nano-SiO₂ and 15% fly ash at 28 days curing period with the increase of steel fibre content. As expected, in general, the addition of steel fibres greatly increased the fracture toughness of HPC containing nano-SiO₂ and fly ash. Both K_{IC}^{ini} and K_{IC}^{un} increased gradually with increase in steel fibre content below 2%. Compared with the HPC reinforced with 0.5% steel fibre, the increase of K_{IC}^{ini} and K_{IC}^{un} was 198% and 168% respectively, for 2% steel fibre content. However, K_{IC}^{ini} and K_{IC}^{un} begin to decrease with the increase in steel fibre content beyond 2%. The variations of K_{IC}^{ini} and K_{IC}^{un} indicate that lesser steel fibre content helps improve the fracture properties of HPC containing nano-SiO₂ and fly ash. With the appropriate dosage, by adding steel fibres to HPC, it was observed that the fractured beam specimens were not separated out because of the bridging of the cracks by steel fibres. Incorporation of fibres in HPC containing nano-SiO₂ and fly ash provided better mechanical integrity during failure. The cracks were bridged across the failure plane and provided some control to the fracture process and thereby the fracture toughness was increased.

Effect of steel fibre on fracture energy

The variations of G_F of steel fibre reinforced HPC containing 5% nano-SiO₂ and 15% fly ash with the steel fibre

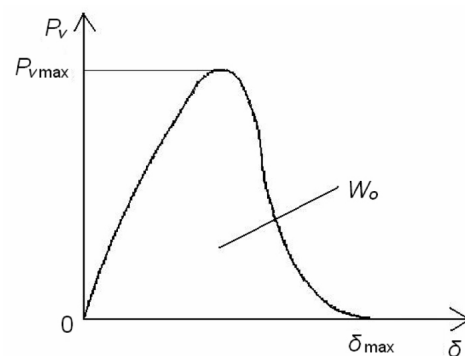


Figure 3. Full curve of $P_V-\delta$.

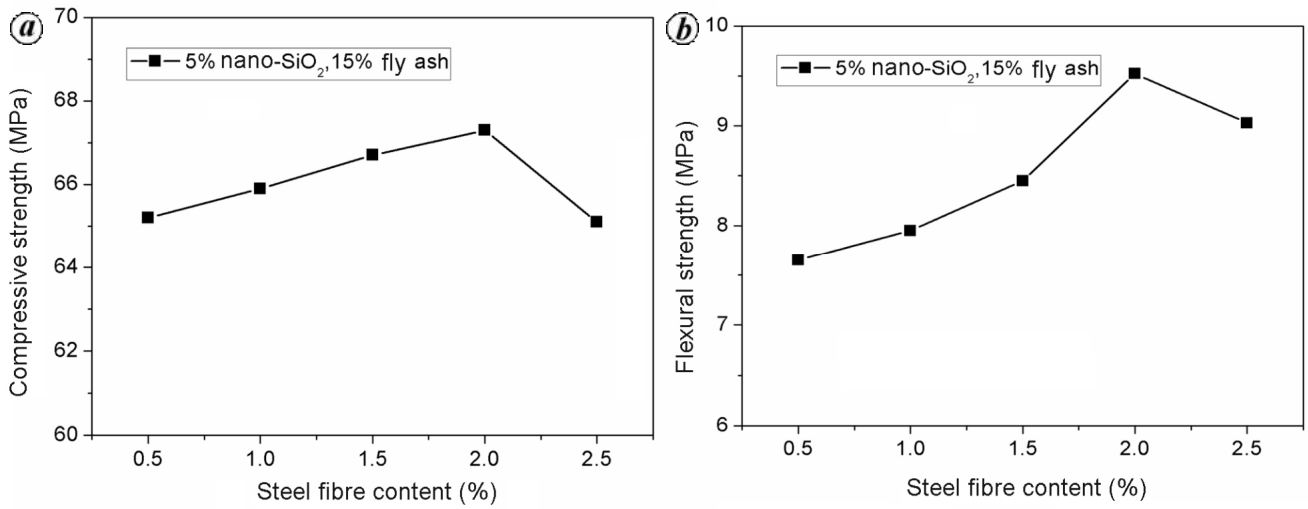


Figure 4. Effect of steel fibre content on (a) compressive strength and (b) flexural strength.

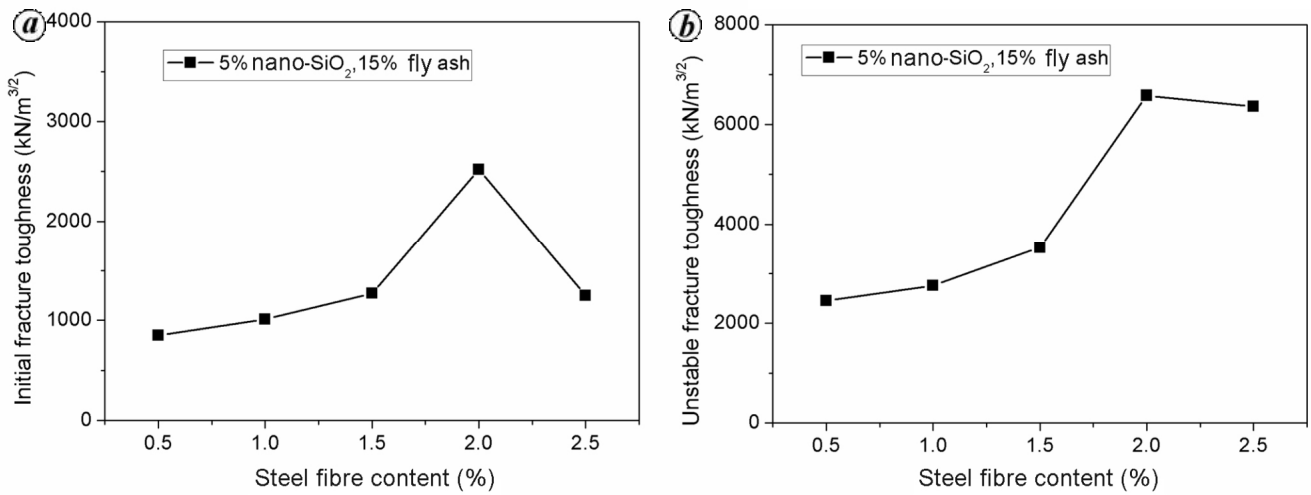


Figure 5. Effect of steel fibre content on (a) initial fracture toughness and (b) unstable fracture toughness.

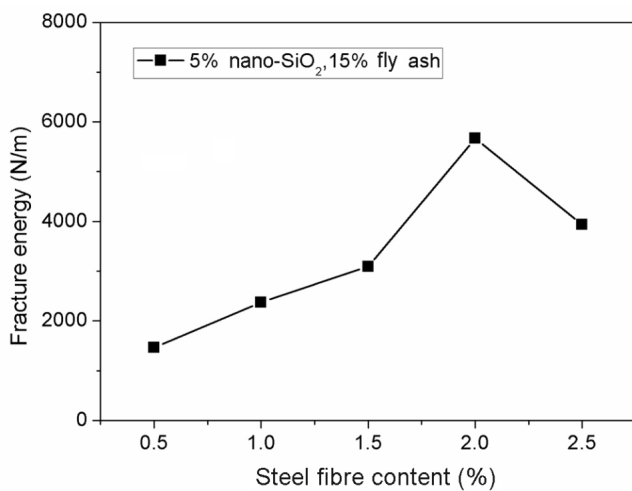


Figure 6. Effect of steel fibre content on fracture energy.

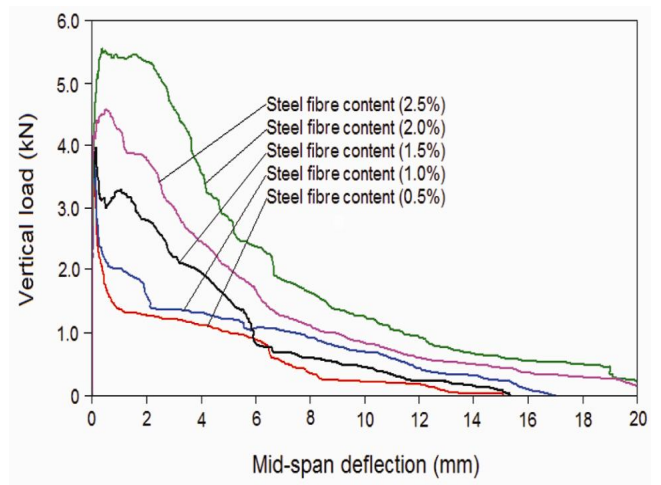


Figure 7. Contrast of P_v-δ curves for different steel fibre contents.

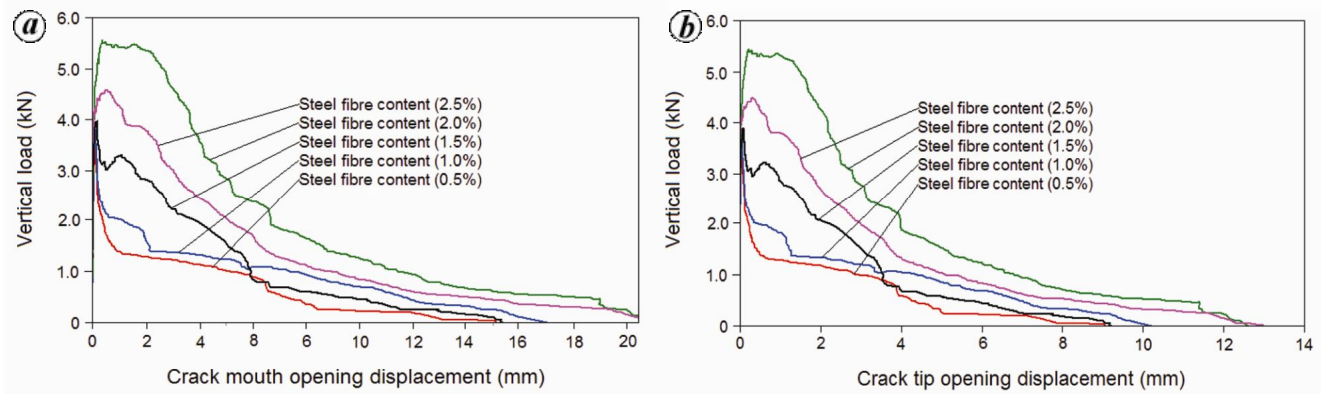


Figure 8. Contrast of (a) P_V -CMOD curves and (b) P_V -CTOD curves for different steel fibre contents.

content increasing from 0.5% to 2.5% at 28 days curing period are shown in Figure 6. There was considerable increase in G_F with increase in steel fibre content up to 2%. Compared with the HPC reinforced with 0.5% steel fibre, the increase in G_F was almost three times with the steel fibre content of 2%. However, as the steel fibre content increases continuously, there was a decrease in G_F . The fracture energy G_F of HPC is a basic material characteristic, representing the energy necessary to create a unit area of fracture surface. The higher G_F indicates that more energy will be consumed to make the HPC fracture and that HPC has better fracture properties. On the contrary, HPC has poor fracture properties with lower G_F . Therefore, the variations of G_F also indicate that lesser steel fibre content helps improve the fracture properties of HPC containing nano-SiO₂ and fly ash.

Figure 7 shows typical complete curves of P_V - δ of the three-point bending beam specimens of HPC containing 5% nano-SiO₂ and 15% fly ash with different contents of steel fibres. It can be seen that the relational curve of P_V - δ becomes thicker and the nonlinear stage of the curve becomes longer, and the descent stage of the curve becomes gentler when the steel fibre content increases from 0.5% to 2%, while the relational curve of P_V - δ becomes thinner when the steel fibre content increases from 2% to 2.5%. For concrete, the thicker and longer relational curve of P_V - δ indicates that the three-point bending beam specimen has better fracture properties³¹. Accordingly, the variation rules of the relational curves of P_V - δ indicate that the resistance to crack propagation of HPC containing nano-SiO₂ and fly ash gradually increases with increase in steel fibre content since the fracture properties improve with steel fibre content less than 2%.

Effect of steel fibre on CMOD and CTOD

The different relational curves of P_V -CMOD and P_V -CTOD of the three-point bending beam specimens of the

HPC containing 5% nano-SiO₂ and 15% fly ash reinforced with different steel fibre contents at 28 days curing period are given in Figure 8a and b respectively. It can be seen that the effect of steel fibre content on the curves is significant, and both the curves become thicker with the increase in steel fibre content from 0.5% to 2%, whereas the curves become thinner when the steel fibre content exceeds 2%.

Figure 9a and b presents the variations of the critical crack opening displacement (CMOD_c and CTOD_c) and the maximum crack opening displacement (CMOD_{max} and CTOD_{max}) respectively of HPC containing nano-SiO₂ and fly ash for different steel fibre contents. CMOD_c can be defined as the crack mouth opening displacement when the vertical load reaches the maximum value³². Similarly, CTOD_c can be defined as the crack tip opening displacement when the vertical load reaches the maximum value. It can be generally seen that the effect of steel fibres on the crack opening displacements is significant, and both CMOD and CTOD increase gradually as the steel fibre content increases from 0.5% to 2.5%. Compared with the HPC reinforced with 0.5% steel fibre, the increase of CMOD_c and CTOD_c was five and six times respectively. It can also be seen that the addition of steel fibres greatly improved the fracture properties of the HPC containing 5% nano-SiO₂ and 15% fly ash. The disordered steel fibres distributing in three dimensions can form a structural support inside the HPC and the strength of the concrete matrix can be improved. Besides, the steel fibres play an important role of bridging microcracks in the concrete composites containing fly ash and nanoparticles, and the cohesive force between the concrete matrix and the steel fibres with high elasticity modulus has a certain anti-cracking effect. Under the loads, some microcracks will appear inside the concrete composites and there will be high stress concentration at the crack tip. When the crack tip reaches the steel fibres, because the strength of the steel fibres is much higher than that of the concrete matrix, and their size is larger than that of the crack tip,

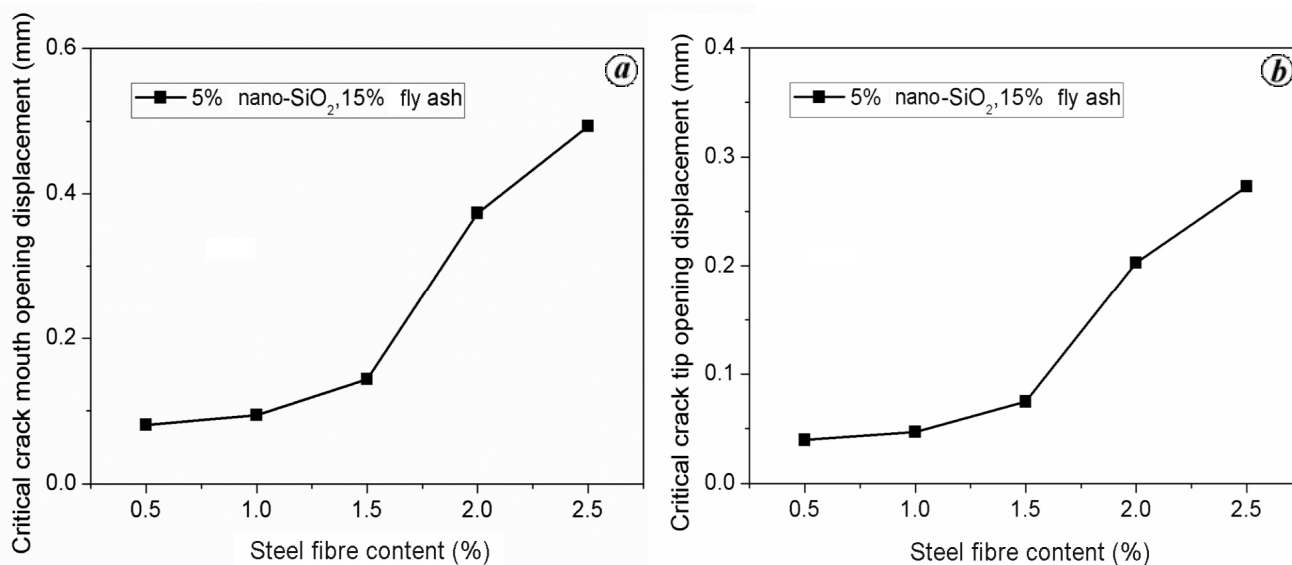


Figure 9. Effect of steel fibre content on (a) critical crack mouth opening displacement and (b) critical crack tip opening displacement.

the steel fibres can prevent the propagation of cracks³³. As a result, with the appropriate fibre content, the addition of steel fibres can improve the fracture properties of HPC containing fly ash and nanoparticles.

Conclusions

We have reported experimental results of fracture property studies conducted on steel fibre reinforced HPC containing nano-SiO₂ and fly ash. The addition of appropriate content of steel fibre helps improve the fracture properties of HPC containing nano-SiO₂ and fly ash. Steel fibre also helps improve the fracture parameters like K_{IC} , G_F , $CMOD_c$ and $CTOD_c$ of HPC. The results also show that steel fibre has a major effect on the relational curves of $P_V-\delta$, P_V-CMOD , and P_V-CTOD of the three-point bending beam specimen. When the steel fibre content increases from 0.5% to 2%, K_{IC} and G_F increase gradually and the fracture relational curves become thicker. However, these fracture parameters begin to decrease and the curves become thinner when the steel fibre content exceeds 2%. The contribution of steel fibre helps improve the fracture properties of HPC containing nano-SiO₂ and fly ash only when its content fibre does not exceed 2%.

1. Yeh, I. C., Modeling of strength of high-performance concrete using artificial neural networks. *Cem. Concr. Res.*, 1998, **28**, 1797–1808.
2. Zhang, P., Li, Q. and Zhang, H., Fracture properties of high-performance concrete containing fly ash. *Proc. Inst. Mech. Eng., Part L: J. Mater.: Des. Appl.*, 2012, **226**, 170–176.
3. Swamy, R. N., *High Performance and Durability Through Design*, ACI Special Publication, 1996, vol. 159, pp. 209–230.

4. Magureanu, C., Sosa, L., Negrutiu, C. and Heghes, B., Mechanical properties and durability of ultra-high-performance concrete. *ACI Mater. J.*, 2012, **109**, 177–184.
5. Elahi, A., Basheer, P. A. M., Nanukuttan, S. V. and Khan, Q. U. Z., Mechanical and durability properties of high performance concretes containing supplementary cementitious materials. *Concr. Build. Mater.*, 2010, **24**, 292–299.
6. Yang, Y. H., Li, Y., Du, X. L. and Wu, Y. S., Mechanical property of self-compacting high performance concrete structure. *J. Beijing Univ. Technol.*, 2010, **36**, 942–947.
7. Muthupriya, P., Subramanian, K. and Vishnuram, B. G., Strength and durability characteristics of high performance concrete. *Int. J. Earth Sci. Eng.*, 2010, **3**, 416–433.
8. Zhang, P. and Li, Q., Fracture properties of high performance concrete containing silica fume. *Aust. J. Struct. Eng.*, 2013, **14**, 320–327.
9. Einsfeld, R. A. and Velasco, M. S. L., Fracture parameters for high-performance concrete. *Cem. Concr. Res.*, 2006, **36**, 576–583.
10. Zhang, P. and Li, Q., Effect of silica fume on durability of concrete composites containing fly ash. *Sci. Eng. Compos. Mater.*, 2013, **20**, 57–65.
11. Lubeck, A., Gastaldini, A. L. G., Barin, D. S. and Siqueira, H. C., Effect of silica fume on durability of concrete composites containing fly ash. *Cem. Concr. Compos.*, 2012, **34**, 392–399.
12. Islam, M. N., Mohd Zain, M. F. and Jamil, M., Prediction of strength and slump of rice husk ash incorporated high-performance concrete. *J. Civ. Eng. Manage.*, 2012, **18**, 310–317.
13. Zhang, P. and Li, Q. F., Durability of high performance concrete composites containing silica fume. *Proc. Inst. Mech. Eng., Part L: J. Mater.: Des. Appl.*, 2013, **227**, 343–349.
14. Salemi, N. and Behfarnia, K., Effect of nano-particles on durability of fibre-reinforced concrete pavement. *Concr. Build. Mater.*, 2013, **48**, 934–941.
15. Said, A. M., Zeidan, M. S., Bassuoni, M. T. and Tian, Y., Properties of concrete incorporating nano-silica. *Concr. Build. Mater.*, 2012, **36**, 838–844.
16. Camiletti, J., Soliman, A. M. and Nehdi, M., Effect of nano-calcium carbonate on early-age properties of ultrahigh-performance concrete. *Mag. Concr. Res.*, 2013, **65**, 297–307.

17. Nazari, A. and Riahi, S., The effect of aluminium oxide nanoparticles on the compressive strength and structure of self-compacting concrete. *Mag. Concr. Res.*, 2012, **64**, 71–82.
18. Nazari, A. and Riahi, S., The effects of TiO₂ nanoparticles on physical, thermal and mechanical properties of concrete using ground granulated blast furnace slag as binder. *Mater. Sci. Eng. A*, 2011, **528**, 2085–2092.
19. Nazari, A. and Riahi, S., The effects of ZnO₂ nanoparticles on properties of concrete using ground granulated blast furnace slag as binder. *Mater. Res.*, 2011, **14**, 299–306.
20. Nazari, A. and Riahi, S., The effects of ZrO₂ nanoparticles on properties of concrete using ground granulated blast furnace slag as binder. *J. Compos. Mater.*, 2012, **46**, 1079–1090.
21. Gopinath, S., Mouli, P. C., Murthy, A. R., Iyer, N. R. and Maheswaran, S., Effect of nano silica on mechanical properties and durability of normal strength concrete. *Arch. Civ. Eng.*, 2012, **58**, 433–444.
22. Zhang, M. H., Islam, J. and Peethamparan, S., Use of nano-silica to increase early strength and reduce setting time of concretes with high volumes of slag. *Cem. Concr. Compos.*, 2012, **34**, 650–662.
23. Givi, A. N., Rashid, S. A., Aziz, F. N. A. and Salleh, M. A. M., Investigations on the development of the permeability properties of binary blended concrete with nano-SiO₂ particles. *J. Compos. Mater.*, 2011, **45**, 1931–1938.
24. Li, G., Use of properties of high-volume fly ash concrete incorporating nano-SiO₂. *Cem. Concr. Res.*, 2004, **34**, 1043–1049.
25. Zhang, P., Li, Q. and Sun, Z., Influence of silica fume and polypropylene fiber on fracture properties of concrete composite containing fly ash. *J. Reinf. Plast. Compos.*, 2011, **30**, 1977–1988.
26. RILEM 50-FMC, Determination of fracture energy of mortar and concrete by means of three-point bend tests on notched beams. *Mater. Struct.*, 1985, **18**, 287–290.
27. Xu, S. and Reinhardt, H. W., A simplified method for determining double-*K* fracture parameters for three-point bending tests. *Int. J. Fract.*, 2000, **104**, 181–209.
28. Xu, S. L., Wu, Z. M. and Ding, S. G., A practical analytical approach to the determination of double-*K* fracture parameters of concrete. *Eng. Mech.*, 2003, **20**, 54–61.
29. Rong, H., Dong, W., Wu, Z. M. and Fan, X. L., Experimental investigation on double-*K* fracture parameters for large initial crack–depth ratio in concrete. *Eng. Mech.*, 2012, **29**, 162–167.
30. Elser, M., Tschegg, E. K., Finger, N. and Stanzl-Tschegg, S. E., Fracture behaviour of polypropylene-fiber-reinforced concrete: modeling and computer simulation. *Compos. Sci. Technol.*, 1996, **56**, 947–956.
31. Yu, Y. Z., Zhang, Y. M., Guo, G. L., Rao, B. and Zhou, J. C., Study on fracture energy G_F of concrete. *Shuli Xuebao*, 1987, **18**, 300–307.
32. Zhang, P., Liu, C. H., Li, Q. F. and Zhang, T. H., Effect of polypropylene fiber on fracture properties of cement treated crushed rock. *Compos. Part B: Eng.*, 2013, **55**, 48–54.
33. Zhang, P., Zhao, Y. N., Liu, C. H., Wang, P. and Zhang, T. H., Combined effect of nano-SiO₂ particles and steel fibers on flexural properties of concrete composite containing fly ash. *Sci. Eng. Compos. Mater.*, 2014, **21**, 1–9.

ACKNOWLEDGEMENTS. We acknowledge the financial support received from the National Natural Science Foundation of China (Grant No. 51208472), open projects funds of the Dike Safety and Disaster Prevention Engineering Technology Research Center of the Chinese Ministry of Water Resources (Grant No. 201201), and the Collaborative Innovation Center of Henan Province of Water Conservancy and Transportation Infrastructure Projects.

Received 8 February 2013; revised accepted 15 February 2014